



## Centrifugal wave-front propagation speed for localizing the atrial tachycardia origin<sup>☆</sup>

Naoya Kurata, Masaharu Masuda<sup>\*</sup>, Mitsutoshi Asai, Osamu Iida, Shin Okamoto, Takayuki Ishihara, Kiyonori Nanto, Takashi Kanda, Takuya Tsujimura, Yasuhiro Matsuda, Shota Okuno, Takuya Ohashi, Akimasa Abe, Toshiaki Mano

Kansai Rosai Hospital Cardiovascular Center, 3-1-69 Inabaso, Amagasaki, Hyogo 660-8511, Japan

### ARTICLE INFO

#### Article history:

Received 2 July 2018

Received in revised form 8 September 2018

Accepted 28 September 2018

Available online 1 October 2018

#### Keywords:

Atrial tachycardia

Centrifugal pattern

Propagation speed

Mapping

### ABSTRACT

**Background:** The earliest activation site (EAS) on a centrifugally-propagated atrial tachycardia (AT) map may represent the true AT origin (true-focal pattern), or the earliest site resulting from passive activation of AT originating from neighboring tissue (pseudo-focal pattern). We assessed the benefits of using the wave-front propagation speed to distinguish between the true- and the pseudo-focal pattern.

**Methods:** AT mapping was performed using a novel ultra-high resolution mapping system with a 64-electrode mini-basket catheter. The true AT origin was defined as the site where radiofrequency application eliminated AT. The wave-front propagation speed was estimated from the area surrounded by the centrifugally-propagated wave front over a specific time interval.

**Results:** Total of 46 centrifugally propagated AT maps from 34 patients were analyzed, including 18 true-focal and 28 pseudo-focal pattern. The area surrounded by the propagated wave front was significantly smaller for the true-focal pattern than for the pseudo-focal pattern, 1–20 msec after the earliest activation. The true-focal pattern was identified by the area 13 msec after the earliest activation, with the best cut-off area value of <4.5 cm<sup>2</sup>.

**Conclusion:** The presence or absence of a true origin of AT at the EAS on centrifugally-propagated AT maps can be distinguished using a wave-front propagation speed.

© 2018 Elsevier B.V. All rights reserved.

## 1. Introduction

Catheter ablation guided by a 3-dimensional (3D) electroanatomical mapping system is established therapy for atrial tachycardia (AT) [1–3]. When the activation map of the AT demonstrates a centrifugal wave-front propagation pattern, radiofrequency application at the earliest activation site (EAS) can eliminate the AT in some cases, but the EAS may simply represent the earliest site resulting from passive activation propagated from neighboring tissue, such as the opposite chamber.

At the moment there is no reliable method to predict whether an EAS will respond to the radiofrequency application or not. The purpose of this study was to investigate whether the centrifugal propagation speeds from EASs on the activation map could be used to distinguish between those cases in which EAS will respond to ablation (cases termed true-focal patterns), and those cases which will not respond to the ablation (cases termed pseudo-focal patterns).

## 2. Methods

### 2.1. Patients

This retrospective study included the data of 46 consecutive centrifugally-propagated AT maps in 39 instances of AT from 34 patients, studied between September 2016 and May 2018. Cases without successful elimination by ablation were excluded, because the true origin could not be determined. This study complied with the Declaration of Helsinki. Written informed consent for the ablation and participation in the study was obtained from all patients, and the protocol was approved by our institutional review board.

### 2.2. AT mapping

Mapping and catheter ablation were performed by two experienced operators (MM and TK), with the patient under intravenous sedation with dexmedetomidine. A 6-Fr decapolar electrode was inserted into the coronary sinus while a second 6-Fr decapolar electrode was placed in the right atrium. A transseptal approach was used for mapping and ablation in the left atrium.

Unless the clinical AT continued at the beginning of the procedure, atrial burst stimuli and/or isoproterenol infusion were used to induce AT. The involved atrium was mapped to detect the AT origin or reentrant circuit according to the activation pattern recorded on the electrode catheter and entrainment pacing. In cases of a centrifugal activation pattern with the EAS localizing to the septum, mapping of the opposite atrium was also performed.

AT mapping using an electroanatomical mapping system (Rhythmia®, Boston Scientific, Marlborough [Cambridge] MA, USA) with a mini-basket array catheter with 64 mini-electrodes (IntellaMap Orion®, Boston Scientific) was performed according to the methods of Mantziari et al. [4] The criteria used for beat acceptance included stable

<sup>☆</sup> All authors take responsibility for all aspects of the reliability and freedom from bias of the data presented and their discussed interpretation.

<sup>\*</sup> Corresponding author.

E-mail address: [masuda-masaharu@kansaiih.johas.go.jp](mailto:masuda-masaharu@kansaiih.johas.go.jp) (M. Masuda).

cycle length, stable timing difference between two reference electrodes placed in the coronary sinus, respiratory gating, stable catheter location, and stable catheter signal compared to adjacent points. The confidence mask and projection distance were set at 0.03 mV and 2 mm, respectively.

### 2.3. Ablation and definition of the true AT origin

Ablation of centrifugally-propagated AT was performed at the EAS during AT. When the AT propagated from both right and left atrial septum, the ablation was initially performed at the septum that demonstrated the earlier activation. An open-irrigated ablation catheter with a 3.5-mm tip (Thermocool Celsius®, Biosense Webster, Diamond Bar CA, USA) via the steerable long sheath was used. Radiofrequency energy was applied for 30 s at each site using a maximum temperature of 42 °C, maximum power of 35 W, and flow rate of 17 mL/min. At the posterior wall near the esophagus, the radiofrequency energy delivery was limited to 15 s, or stopped when the esophageal temperature monitored with an esophageal probe (SensiTherm®, St. Jude Medical) reached 40 °C. If AT was terminated by radiofrequency application, AT induction by atrial burst stimuli and/or isoproterenol infusion was repeated. The procedural endpoint was no inducibility of any stable ATs. The AT origin was defined as the site where the radiofrequency application successfully terminated the AT, and eliminated AT inducibility.

### 2.4. Measuring the area surrounded by the propagation wave front

Using the data from the ablation sessions, we assessed the centrifugal propagation speed by measuring the area surrounded by the propagation wave front on the map (Fig. 1) every msec after the earliest activation up to 20 msec. Each propagation area was depicted by adjusting the activation color circle as setting the beginning of “early meets late” (the color spectrum of deep red between purple and red) at the time of earliest

atrial activation and then incrementing the duration by 1 msec to 20 msec. The area was measured by manually tracing the border of “early meets late.”

### 2.5. Statistical analysis

Continuous data are expressed as the mean  $\pm$  standard deviation or median (interquartile range). Categorical data are presented as absolute values and percentages. Tests for significance were conducted using the unpaired *t*-test for continuous variables with normal distribution, and the Wilcoxon rank sum tests for continuous variables with non-normal distribution. The chi-squared test or Fisher's exact test were used for comparing categorical variables. For the prediction of the location of the true origin at the EAS, a receiver operating characteristic (ROC) curve was constructed for the area surrounded by the wave-front propagation. The area under the curve (AUC) was determined and a 95% confidence interval (CI) for the AUC was calculated using the bootstrap method. To assess correlations between the continuous variables, Pearson's correlation coefficient analysis was performed. All analyses were performed using SPSS version 20.0 software (SPSS, Inc., Chicago IL, USA).

## 3. Results

### 3.1. Baseline characteristics

Patient characteristics are shown in Table 1. Most of the patients had atrial fibrillation and had undergone pulmonary vein isolation. During the procedures, 46 centrifugally-propagated AT maps were created for 39 AT episodes.

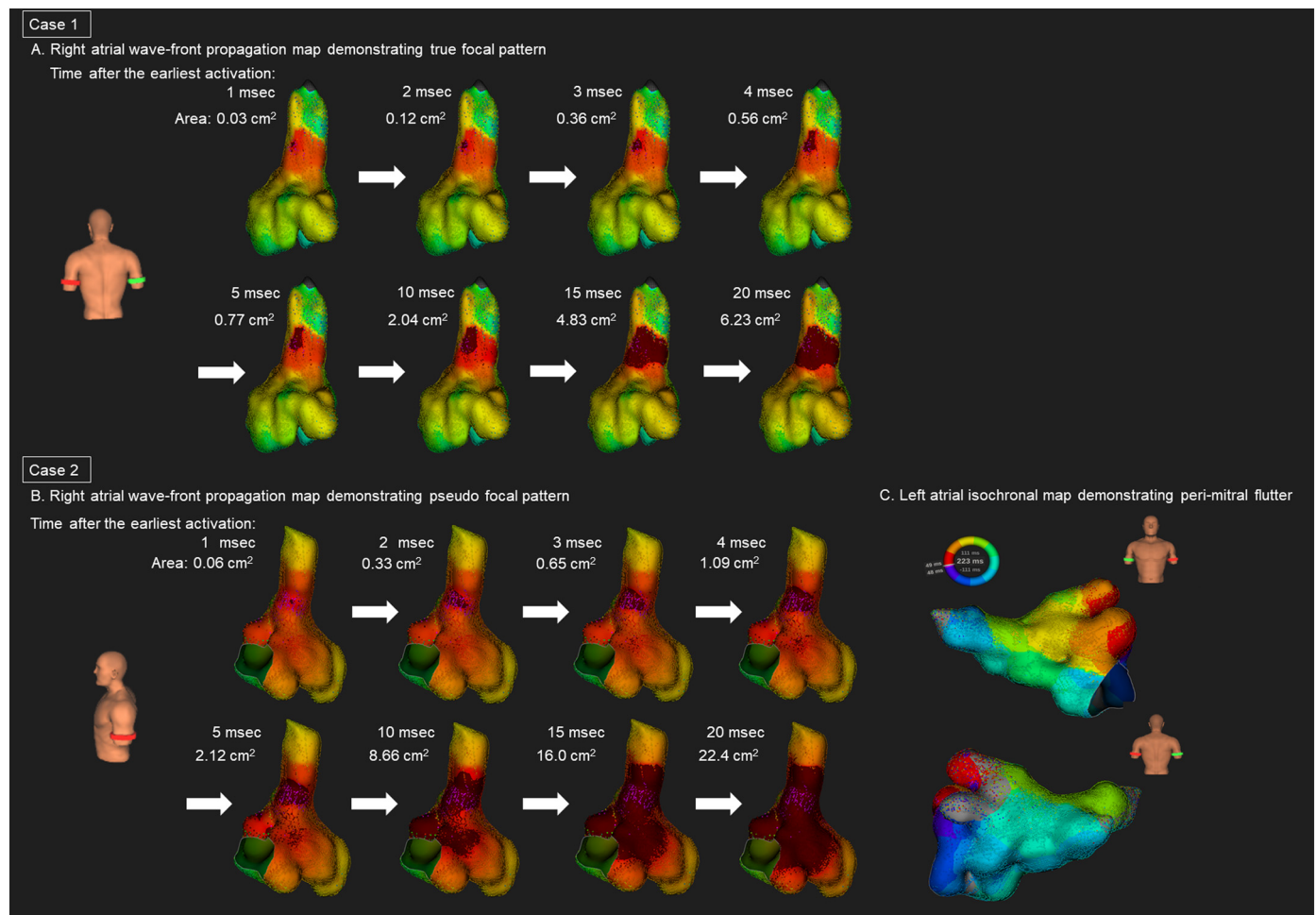


**Fig. 1.** Representative cases. A measured area surrounded by propagated wave front is shown at each time point after the earliest activation. The wave-front propagation speed is slower on the propagation map in case 1 (the true focal pattern, A) than that in case 2 (the pseudo focal pattern, B). In case 2, Left atrial perimitral AT (C) was propagated to the right atrium.

**Table 1**  
Patient characteristics.

Variables	N = 34
Age, years	70 ± 9
Male, n (%)	14 (41)
Body mass index, kg/m <sup>2</sup>	22.3 ± 3.5
Atrial fibrillation, n (%)	29 (85)
CHADS <sub>2</sub> -VA <sub>2</sub> Sc score	2.1 ± 1.2
Left atrial diameter, mm	42 ± 7
Previous cardiac surgery, n (%)	3 (9)

### 3.2. Characteristics of each AT map

Mapping was performed in the right (n = 28 [61%]) and left atrium (n = 18 [39%]) with mean acquired points = 10,829 ± 7963. The mean tachycardia cycle length was 303 ± 84 msec. Using the data on response to ablation, we found that the centrifugal propagation maps showed the true-focal pattern in 18 (39%) maps and the pseudo-focal pattern in 28 (61%). The ATs with the pseudo-focal pattern on the initial propagation map were focal ATs (n = 8) and macro-reentrant ATs (n = 20) in the neighboring chambers. Representative cases are presented in Fig. 1. Detailed information on each AT map is presented in Supplementary table.

Comparisons of electrophysiological characteristics between AT maps with the true- and pseudo-focal patterns are shown in Table 2. There were no difference in the ablation lesions prior to AT mapping between 2 groups. AT with the true-focal pattern had longer cycle length than that with the pseudo-focal pattern. Frequencies of QS morphology on the uni-polar recording at the EAS were not different between 2 groups.

### 3.3. Area surrounded by the wave-front propagation

Fig. 2 shows the areas surrounded by propagated wave front at 5, 10, 15, and 20 msec after the earliest atrial activation. The area was significantly smaller in the true-focal pattern than in the pseudo-focal pattern at every time point between 1 and 20 msec. ROC curve analysis revealed that a time of 13 msec after the earliest activation best differentiated the true-focal from the pseudo-focal pattern with an AUC of 0.972. The best cut-off value of the area surrounded by the propagated wave front was

4.5 cm<sup>2</sup>, yielding a sensitivity of 96%, a specificity of 95%, and predictive accuracy of 96%.

A scatter gram (Supplementary figure) demonstrates that the cut-off value of 4.5 cm<sup>2</sup> well differentiated the true- and the pseudo-focal patterns in most of ATs. The area surrounded by propagated wave front did not correlate with AT cycle length.

## 4. Discussion

This retrospective study included 46 AT maps demonstrating a centrifugal wave-front propagation in 39 ATs from 34 patients. Centrifugal propagation maps displayed the true-focal pattern in 18 (39%) and the pseudo-focal pattern in 28 (61%) instances. Main findings were as follows: [1] centrifugal propagation speeds between 1 and 20 msec after the earliest activation were slower in the true-focal pattern than in the pseudo-focal pattern. [2] The area surrounded by the propagated wave front at 13 msec after the earliest activation best differentiated the true-focal from the pseudo-focal pattern, with the best cut-off area = 4.5 cm<sup>2</sup>.

### 4.1. AT origin and wave-front propagation speed

A slower centrifugal wave-front propagation speed in case of the EAS being the true AT origin compared with that of the EAS not being the AT origin would be partially explained by the different propagation patterns as follows: A true-focal AT originating from atrial endocardium would radiate outward in concentric circles to cover the atrial endocardial surface. In the case of the pseudo-focal pattern where AT originated from the neighboring chamber, the activation wave front would propagate though some connections radially in a spherical pattern, and be projected to the atrial endocardium [5,6]. Assuming that the 3-dimensional propagation speeds were identical, the 2-dimensional spreading speed on the atrial endocardium becomes slower in the true-focal pattern.

However, the local tissue conduction properties and coupling interval (AT cycle length) around the EAS could significantly influence the wave-front propagation speed. Therefore, we have to realize that a universal cut-off value of the area surrounded by the wave-front propagation would not always differentiate a true focal AT from a pseudo focal AT.

### 4.2. Clinical implications

Utilizing the propagation speed for the identification of the true AT origin from a centrifugally propagated AT map would be very helpful in the clinical setting, because no additional procedural maneuver in the heart is required. Conversely, conventional diagnostic methods, such as entrainment pacing and mapping in the neighboring chamber, are not only time-consuming but may also change or terminate the target AT [7,8].

### 4.3. Limitations

Several limitations of this study warrant mention. The results represent a single center's experience, which might be operator-dependent. Mapping using the mini basket catheter may have failed to draw the entire endocardial surface in the atria, possibly resulting in the incorrect localization of EAS and/or propagation areas. The AT origin estimated by the response to the radiofrequency application might not necessarily be correct, because conductive heating from the radiofrequency application could injure the neighboring tissue near the radiofrequency application site. Next, an unblinded study design could bias the results. In addition, relatively restrictive beat acceptance criteria limit the versatility of the study results. Another limitation is that the statistical analyses might have been influenced by the relatively small size of the study population. Multicenter

**Table 2**  
Electrophysiological characteristics.

	True-focal n = 18	Pseudo-focal n = 28	p
Mapped chamber			
Left atrium, n (%)	10 (56%)	8 (29%)	0.07
Right atrium, n (%)	8 (44%)	20 (71%)	
Ablation lesions created before atrial tachycardia mapping			
Pulmonary vein isolation, n (%)	15 (83%)	25 (83%)	0.57
Linear ablation, n (%)			
Left atrial anterior or septal, n (%)	8 (29%)	2 (44%)	0.17
Left atrial Roof, n (%)	6 (33%)	12 (43%)	0.53
Bottom, n (%)	4 (18%)	4 (18%)	0.72
Posterior mitral isthmus, n (%)	3 (17%)	1 (4%)	0.13
Cavo-tricuspid isthmus, n (%)	6 (33%)	8 (29%)	0.74
Low-voltage ablation, n (%)			
Left atrium, n (%)	8 (47%)	9 (32%)	0.33
Right atrium, n (%)	1 (6%)	0	0.22
Non-pulmonary-vein trigger ablation, n (%)			
Superior-vena cava isolation, n (%)	0	1 (4%)	0.43
Left atrium, n (%)	2 (11%)	4 (14%)	0.76
Right atrium, n (%)	3 (17%)	3 (11%)	0.57
Tachycardia cycle length, ms	338 ± 98	283 ± 68	0.03
QS pattern on the uni-polar electrogram at the earliest activation site, n (%)	10 (67%)	13 (48%)	0.26

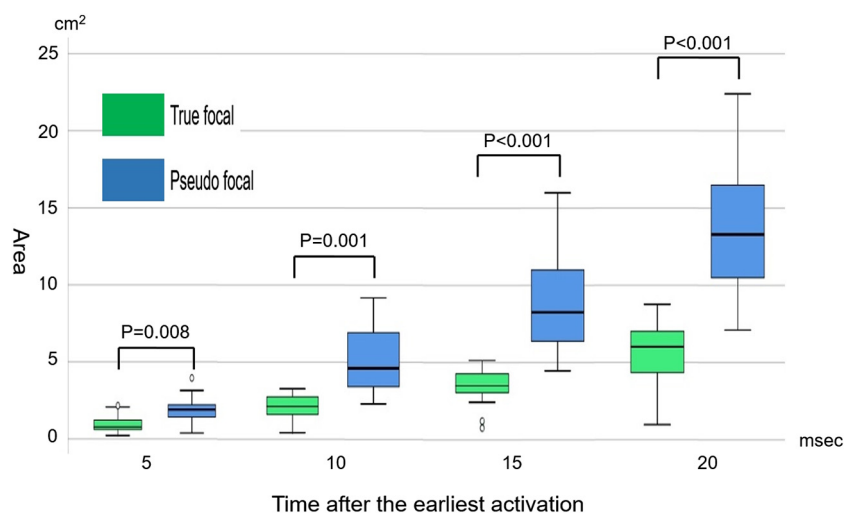


**Fig. 2.** Comparison of the areas surrounded by propagated wave front between the true-focal and pseudo-focal patterns at 5, 10, 15, and 20 msec after the earliest activation. The areas surrounded by propagated wave front were significantly smaller in the true-focal pattern than in the pseudo-focal pattern. The horizontal lines within the box indicate the median, boundaries of the box indicate the 1st and 3rd quartiles, and the whiskers indicate the 5 and 95 percentiles. Points below and above the whiskers are drawn as individual points.

studies including larger populations are needed to make conclusions about the general usefulness of this method.

## 5. Conclusion

The existence or absence of the AT origin at the EAS on AT map demonstrating centrifugal activation pattern may be differentiated using the centrifugal wave-front propagation speed.

Supplementary data to this article can be found online at <https://doi.org/10.1016/j.ijcard.2018.09.117>.

## Conflict of interest

None.

## Grant support

None.

## References

- [1] S.A. Chen, C.E. Chiang, C.J. Yang, et al., Sustained atrial tachycardia in adult patients. Electrophysiological characteristics, pharmacological response, possible mechanisms, and effects of radiofrequency ablation, *Circulation* 90 (1994) 1262–1278.
- [2] Lesh Md, G.F. Van Hare, L.M. Epstein, et al., Radiofrequency catheter ablation of atrial arrhythmias. Results and mechanisms, *Circulation* 89 (1994) 1074–1089.
- [3] E.P. Walsh, J.P. Saul, J.E. Hulse, et al., Transcatheter ablation of ectopic atrial tachycardia in young patients using radiofrequency current, *Circulation* 86 (1992) 1138–1146.
- [4] L. Mantziari, C. Butcher, A. Kontogeorgis, et al., Utility of a novel rapid high-resolution mapping system in the catheter ablation of arrhythmias. An initial human experience of mapping the atria and the left ventricle, *JACC Clin. Electrophysiol.* 1 (2015) 411–420.
- [5] M. Chauvin, D.C. Shah, M. Haïssaguerre, L. Marcellin, C. Brechenmacher, The anatomic basis of connections between the coronary sinus musculature and the left atrium in humans, *Circulation* 6 (2000) 647–652.
- [6] S. Sakamoto, T. Nitta, Y. Ishii, Y. Miyagi, H. Ohmori, K. Shimizu, Interatrial electrical connections: the precise location and preferential conduction, *J. Cardiovasc. Electrophysiol.* 10 (2005) 1077–1086.
- [7] T. Rostock, I. Drewitz, D. Stevem, et al., Characterization, mapping, and catheter ablation of recurrent atrial tachycardias after stepwise ablation of long-lasting persistent atrial fibrillation, *Circ. Arrhythm. Electrophysiol.* 3 (2010) 160–169.
- [8] M. Estato, G. Hindricks, P. Sommer, et al., Color-coded three-dimensional entrainment mapping for analysis and treatment of atrial macroreentrant tachycardia, *Heart Rhythm.* 6 (2009) 349–358.